Combined experimental and molecular dynamics investigation of 1D rod-like asphaltene aggregation in toluene-hexane mixture

Kundarapu, Laxman Kumar; Choudhury, Satyajeet; Acharya, Sriprasad; Vatti, Anoop Kishore; Pandiyan, Sudharsan; Gadag, Shivaprasad; Nayak, Usha Yogendra; Dey, Poulumi

DOI
10.1016/j.molliq.2021.116812

Publication date
2021

Document Version
Final published version

Published in
Journal of Molecular Liquids

Journal of Molecular Liquids 339 (2021) 116812

Contents lists available at ScienceDirect

Journal of Molecular Liquids

journal homepage: www.elsevier.com/locate/molliq

Combined experimental and molecular dynamics investigation of 1D rod-like asphaltene aggregation in toluene-hexane mixture

Laxman Kumar Kundarapu [a], Satyajeet Choudhury [a], Sriprasad Acharya [a], Anoop Kishore Vatti [a,*], Sudharsan Pandiyan [b], Shivaprasad Gadag [c], Usha Yogendra Nayak [c], Poulumi Dey [d,*]

[a] Department of Chemical Engineering, Manipal Institute of Technology (MIT), Manipal Academy of Higher Education (MAHE), Manipal, Karnataka 576104, India
[b] Schrödinger, Bengaluru, Karnataka 560086, India
[c] Department of Pharmaceutics, Manipal College of Pharmaceutical Sciences, Manipal Academy of Higher Education (MAHE), Manipal, Karnataka 576104, India
[d] Department of Materials Science and Engineering, Faculty of Mechanical, Maritime and Materials Engineering, Delft University of Technology, 2628 CD Delft, the Netherlands

ARTICLE INFO

Article history:
Received 28 April 2021
Revised 13 June 2021
Accepted 22 June 2021
Available online 10 July 2021

Keywords:
1D Rod-like Aggregates
Optical Microscopy
FTIR
MD Simulations
Density Contours

ABSTRACT

The aggregation behavior of asphaltene in the toluene-hexane mixture is systematically investigated using experimental techniques such as optical microscopy and Fourier-transform infrared spectroscopy (FTIR) combined with molecular dynamics (MD) simulations. The optical images of various asphaltene concentrations are processed to determine the size of asphaltene aggregates. FTIR is performed within our work in order to understand the formation of aggregates and its interaction with the solvent mixture. MD simulations are employed to achieve atomistic insights into the aggregation behavior of asphaltene. The end-to-end distance of the asphaltene molecule is calculated for various asphaltene concentrations in the toluene-hexane mixture. The dynamical properties of the asphaltene aggregates such as the diffusion coefficient and shear viscosity are calculated. Further, an in-depth analysis of the density contours is performed to probe the clusterization of asphaltene. Thus obtained structural and dynamical properties of the asphaltene aggregates in the toluene-hexane mixture are compared with our experimental findings. Our results thereby highlight the importance of the combined experimental and theoretical study to achieve deeper and better insights into the aggregation behavior of asphaltene in toluene-hexane mixture.

1. Introduction

Asphaltene is one of the most important ingredients of crude oil together with saturates, resins and aromatics. It is the heaviest component of the crude oil and holds the highest fraction [1] consisting of aliphatic chains, polycyclic aromatic hydrocarbons and polar-hetero atoms [2]. Asphaltenes can be dissolved in aromatic solvents like toluene, benzene and pyridine but are insoluble in normal alkanes like pentane, hexane and heptane [3,4]. Asphaltenes form aggregates in normal alkanes, water and oil–water emulsion [5] and are responsible for the high viscosity of crude petroleum [6,7]. Destabilized asphaltenes cause numerous problems in the transportation of heavy oils, catalyst deactivation, emulsion destabilization etc. [8,9,7]. It has a severe impact in petroleum productivity due to high viscosity in crude oil caused by its presence [10,11]. Also, the release of asphaltenes into the aqueous environment can have drastic effect on aquatic life and soil because of their not-decaying nature [12,13].

A better understanding of the asphaltene aggregation is a key to design efficient oil recovery mechanisms [14]. Numerous experimental studies and theoretical investigations have been conducted to probe the asphaltene aggregation mechanisms and the nature of the aggregates in various solvents [15–17,14]. The widely accepted Yen-Mullins model reveals that the asphaltene molecules tend to form nanoaggregates when their number is below 10. Further, these nanoaggregates adhere together to form the macroaggregates [18,19,15]. This model also suggests that the polyaromatic core is surrounded by the aliphatic side chains and the π-π interactions between the polyaromatic cores are responsible for the aggregation [20].

Mullins et al. [15] discussed various critical aspects related to asphaltene such as their molecular structure and the aggregation of nanoaggregates to form clusters. The equation of state to investigate oil field reservoir's asphaltene gradients has been implemented for the various types of crude oil reservoirs such as condensates, black oil, and heavy oil. Further, the analysis of the

* Corresponding authors.
E-mail addresses: anoop.vatti@manipal.edu (A.K. Vatti), p.dey@tudelft.nl (P. Dey).

https://doi.org/10.1016/j.molliq.2021.116812
0167-7322/

unimolecular decomposition revealed that a single polycyclic aromatic hydrocarbon favors island type of molecular architecture. Aslan et al. [21] performed flow-line experiments on 1 mm stainless steel conduit to study the water-asphaltene interactions. The size of asphaltene aggregates is measured using differential interference contrast microscopy and dynamic light scattering techniques. The viscosity of solutions are investigated using the rheometer by varying the concentration of deionized water in petroleum fluids. In their work, the hydrogen bonds between the asphaltene and water are extensively analyzed. Cyran et al. [22] probed the structure of polycyclic aromatic hydrocarbon compounds, i.e., Violanthrone-79 and anthrone using 2D infrared spectroscopy. The spectral region of 1550–1700 cm^{-1} is investigated to probe the carbonyl stretching for understanding the effect of solvent on aggregation. The molecular structure of asphaltene aggregates is characterized using the atomic force and scanning tunneling microscopy techniques by Schuler et al. [23]. Zhang et al. [24] probed the asphaltene molecular interactions in weight ratio of toluene to heptane using the surface forces apparatus (SFA).

Li et al. [17] investigated the asphaltene aggregation kinetics in the capillary tubes. The aggregate size and its distribution versus flocculation time are analyzed at various concentrations of asphaltene. Further, in their work, the diffusion-limited-aggregation and reaction-limited-aggregation models are systematically analyzed. Duran et al. [25] performed size and fractal measurements of asphaltene aggregates using micrographic methods and focused beam reflectance at different n-heptane concentrations. In their work, the micrographic images and the fractal measurements revealed close-packed linear and planar aggregate structures at the onset of precipitation. Further, it is observed that the asphaltene aggregates remain closely packed.

Headen et al. [19] investigated the radial distribution function of asphaltenes aggregates and resins in heptane and toluene solvents using MD simulations. It is observed that dimers and trimers of aggregates in toluene solvent are formed, broken and once gain formed with other molecules. Santos et al. [26] performed MD simulations on asphaltene in toluene, heptane and water and also investigated asphaltene aggregation in binary and ternary solvent mixture. The effect of the lateral side chains is investigated in detail in this study. MD simulations were also performed by Jian et al. [27] on Violanthrone-78 based asphaltene model with different ratios of aliphatic and aromatic ratios in toluene solution. The study concluded that the π-π interactions between polyaromatic cores play a key role for asphaltene aggregation. Further, it is found that both the aliphatic and aromatic regions of asphaltenes show attractive interactions in contrast to water. Jian et al. [28] investigated four representative polyaromatic compounds in a mixture of toluene and n-heptane using MD simulations. The study showed that single type of polyaromatic compound form short cylinder-like aggregates in parallel stacking arrangement leading to the formation of one-dimensional (1D) rod-like structure. Wang et al. [29] performed coarse-grained modeling of three different asphaltene molecular structures. Their results explain the formation of 1D rod-like aggregates followed by the formation of the nanoaggregates.

Bian et al. [30] investigated the disaggregation of asphaltenes using experimental and atomistic techniques viz. MD and quantum chemical simulations. It is concluded from this study that methylation favours disaggregation of asphaltene aggregates by increasing the distance between π-π stacks. Tirjoo et al. [31] studied asphaltene aggregation for two different asphaltene models with one containing two lateral side chains and the other containing two methyl groups. Recently, Soulgani et al. [32] studied asphaltene aggregation in toluene and n-hexane mixture by performing experiments and theoretical investigation using hydrodynamic modeling. The aggregate sizes in solution are investigated using optical microscopy and the settling time of the aggregates is calculated. In their work, the mechanism of asphaltene aggregation is investigated by both general reaction-limited and diffusion-limited aggregation theories.

In the present work, we present an in-depth analysis of the 1D rod-like asphaltene aggregation in toluene-hexane mixture combining experiments and MD simulations for the first time in the literature. The optical images of the asphaltene aggregates and the Fourier-transform infrared spectroscopy (FTIR) spectra of the aggregates in solution are analysed. We report the viscosity of the asphaltene molecules in toluene and hexane mixture for the first time to the best of our knowledge. We have also calculated end-to-end distance and diffusion coefficient of the asphaltene molecules in toluene and hexane mixtures. Furthermore, we have analyzed the time averaged density contour of the aggregates to achieve a deeper understanding of the aggregate position and the nature of interaction.

2. Experimental details

In this study, one of the model compounds of asphaltene, Violanthrone-79, is used for the investigations of asphaltene aggregation. Amorphous Violanthrone-79 with purity up to 95% is procured from BLD Pharmatech Limited. Based on the Hansen solubility results of earlier work [33], toluene and n-hexane are selected as the solvent and precipitating titrant, respectively. Four samples of asphaltene of different weights, (i.e. 0.02 g to 0.08 g) are considered for the study. Toluene is added to asphaltene till it dissolves completely. This is considered as the base solution for the study. Titrant, n-hexane, is added to this solution incrementally (starting from 0.1 mL) till the formation of aggregates is observed. Starting from the base solution, the asphaltene at every concentration of titrant is thoroughly mixed to ensure that the asphaltene particles are uniformly distributed. The aggregation phenomenon at different concentrations of titrant has been investigated using two methods, the filter paper method [34] and the microscopic method [17,32]. In the filter paper method, Whatman grade 41 filter paper is used to observe the aggregation phenomenon. At every concentration of the titrant, 20 μL solution is pipetted out and dropped on the filter paper. The solution spreads on the filter paper and creates a spot. The created spots at different concentrations of titrant are observed for notable changes, like a ring with asphaltene particles. The solutions at these different concentrations are transferred to petri dishes to capture the images. Further, the petri dishes are covered with lid to prevent the vaporization of solvent and the titrant. The images are captured using inverted microscope, Olympus IX73, and the microscopic images are analysed for the size distribution of the aggregates. Fourier Transform Infrared Spectroscopy (FTIR) characterization is carried out using FT/IR-6300 (Jasco). Herein, the samples are scanned in the wavenumber range of 400 to 4000 cm^{-1} with a scanning resolution of 0.07 cm^{-1}.

3. Computational Details

Violanthrone-79 ($C_{50}H_{48}O_4$) asphaltene model has a molecular weight of 712.9 g/mol. It contains nine aromatic rings, two linear aliphatic side groups, and four oxygen heteroatoms in the polyaromatic core of the molecule as shown in Fig. 1. In addition, toluene and hexane explicit molecules are considered as organic solvent mixture. The bonded and Lennard-Jones interactions in the simulated systems studied are described using the Optimized Parameters for Liquid Simulations (OPLS3e) [35] force field. The Desmond [36] package within Schrödinger simulation software [37] is used to perform the molecular dynamics simulations. The

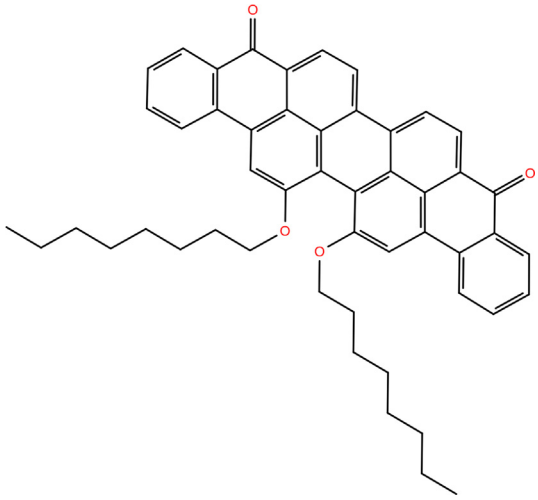

Fig. 1. 2-dimensional structure of the asphaltene model compound, i.e.,Violanthrone-79 considered within this study. Aromatic core, polar-hetero-atoms, i.e., oxygen and two side chains are shown.

equations of motion are integrated with a time step of 2 fs. Nose–Hoover thermostat is used, and non-bonded interactions are truncated at 9 Å. We have considered three different concentrations viz. 12, 36, and 60 of asphaltene molecules in toluene and hexane mixture as shown in Table 1. The toluene to hexane weight ratios for the 12, 36, and 60 asphaltene molecules are 0.64, 0.76, and 0.9, respectively. Snapshots of the asphaltene aggregation for 36 asphaltene molecules in hexane and toluene mixture before and after aggregation collected at 0.07 ns and 9.19 ns time frames are shown in Fig. 2.

4. Results and Discussion

4.1. Optical Microscopy

We have analyzed three key steps of the aggregation process, i.e., asphaltene particles formation (before on-set), the on-set of aggregation (at on-set), excess aggregation (after on-set) using the optical microscope. The concentrations of n-hexane are observed as 4, 12 and 22 vol.% at the three key steps for 0.06 g of asphaltene in the solution. Fig. 3 shows the microscopic images at the key steps respectively for 0.06 g of asphaltene in the solution. In Fig. 3(a), an optical image of the base solution is shown for comparison of the case when there are no aggregates in solution to the one where there are large size aggregates in the solution. In Fig. 3(b), the aggregates start to form at 4 vol.% hexane concentration. It is evident from the figure that the separation of the asphaltene particles from toluene increases with increase in the concentration of the titrant. The aggregates are observed to be directional in nature at the lower concentration of the asphaltenes. The formation of aggregates from separated particles is thus well explained by our experimental study as evident in Fig. 3(c), where a pure polyaromatic asphaltene compound is observed to form 1D rod-like structures. With further addition of n-hexane, we observed cylinder-like aggregates as shown in Fig. 3(d), with no preferred stacking direction. This observation is well supported by our MD simulations as evident from the snapshot of a single aggregate as shown in Fig. 4. Further, a clear stacking arrangement of the single aggregate, where π-π interactions domination can be seen in the figure.

Table 1
The number of asphaltene, toluene and hexane molecules are presented in the table below for three different asphaltene concentrations.

Asphaltene molecules	Toluene molecules	Hexane molecules	Simulation box size (Å^3)
12	1500	2488	93.8×93.8×93.8
36	1652	2312	94.2×94.2×94.2
60	1804	2136	94.6×94.6×94.6

In order to increase the accuracy of the image analysis, several images are captured at each level of titrant concentration. These images are analysed to check the intensity of aggregates formation in terms of length, thickness, and the number of asphaltene particles at the key steps. The image analysis of 0.06 g asphaltene in solution is presented in Table 2. The obtained results clearly show that the length, thickness, and the number of asphaltene particles increase with the increase in the titrant concentration. The major difference between the on-set and after on-set images is the thickness of particles, i.e., 6.55 μm and 10.86 μm for the on-set and after on-set images respectively.

We have calculated the total area of the aggregates and the average length and thickness of the particles using ImageJ analysis [38]. The approximate total number of particles is calculated using the following Eq. 1.

$$\text{Total number of particles} = \frac{\text{total area of all the aggregates}}{\text{average particle area of aggregate}} \quad (1)$$

It is important to note that few particles overlap in Figs. 3(c) and 3(d). To account for the overlapping particles, we have assumed 15–30 % excess total area for all the aggregates in Figs. 3(c) and 3(d). The approximate number of particles before on-set, at on-set and after on-set are found to be 45, 83 and 100 respectively. Moreover, using this quantitative analysis, it can be explained that the increase in the titrant concentration increases the number of particles.

4.2. Fourier Transform Infrared Spectroscopy (FTIR)

The FTIR spectra of the four samples under investigation are shown in Fig. 5. This technique provides information about the functional group associated with a molecular bond, and the peaks at different wavenumbers show the type of bonds. The red line in the Fig. 5 indicates the spectra for the fully dissolved asphaltene in toluene. The green line indicates the spectra for the asphaltene-toluene mixture along with hexane, where on-set of the aggregation is observed. The blue line represents the spectra for the asphaltene-toluene mixture together with higher amount of hexane, where the aggregates are clearly visible and the orange line is the spectra for the pure asphaltene compound. The sharp peak located at around 3100 cm^{-1} is assigned to the aromatic C-H stretch and the one at 2910 cm^{-1} to the asymmetric C-H stretch. The small peak observed at 2850 cm^{-1} is due to symmetric CH_3 stretch. Most importantly, carbonyl stretching (C = O) is in the range of 1700–1550 cm^{-1}. Further, 1600 cm^{-1} is for conjugated C = C, 1570 cm^{-1} for aromatic ring stretching C = C-C, 1480 cm^{-1} for the asymmetric CH_3 bend, 1380 cm^{-1} for symmetric CH_3 bend, 1080–1020 cm^{-1} for alkyl substituted C-O stretch, and finally, at 750–700 cm^{-1} for the mono substituted aromatic ring C-H (toluene). The deepest peak is observed at 750–700 cm^{-1} where aggregates are pronounced and clearly visible in the solution, thereby providing clear indication of the separation of the asphaltene particles from toluene.

The infrared spectra provide insights into the vibrational modes which are coupled in the aggregates. The carbonyl stretching mode can be critical in understanding the aggregation behavior using the infrared spectra. We observe a clear change in the peak intensity in

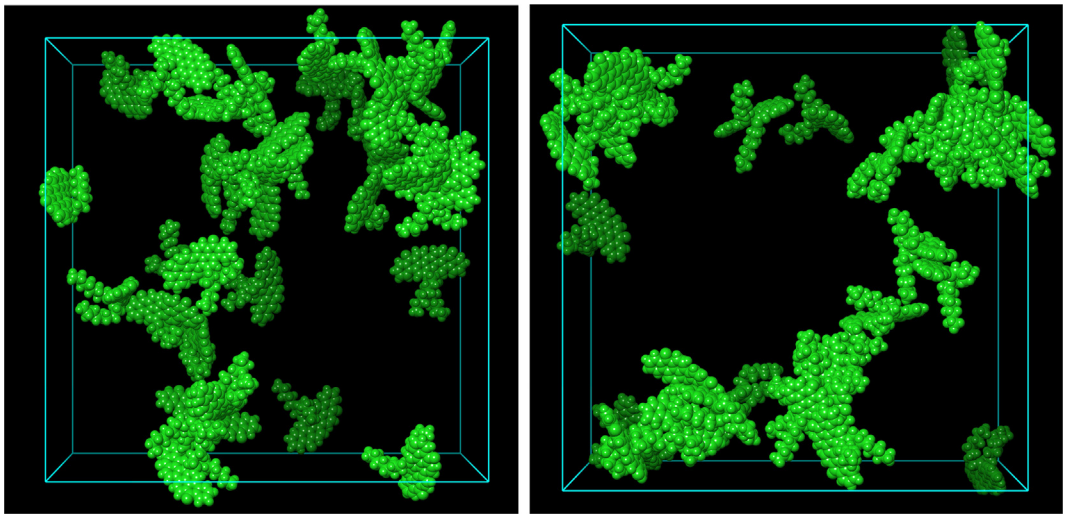

Fig. 2. Initial (left) and final (right) snapshots of the MD run of asphaltene aggregates in toluene-hexane mixture are shown for 36 asphaltene molecules. The initial and final snapshots are for 0.07 ns and 9.19 ns time frames, respectively. For the clear visibility of aggregates, only asphaltene aggregates (green) are shown and hexane-toluene molecules are hidden.

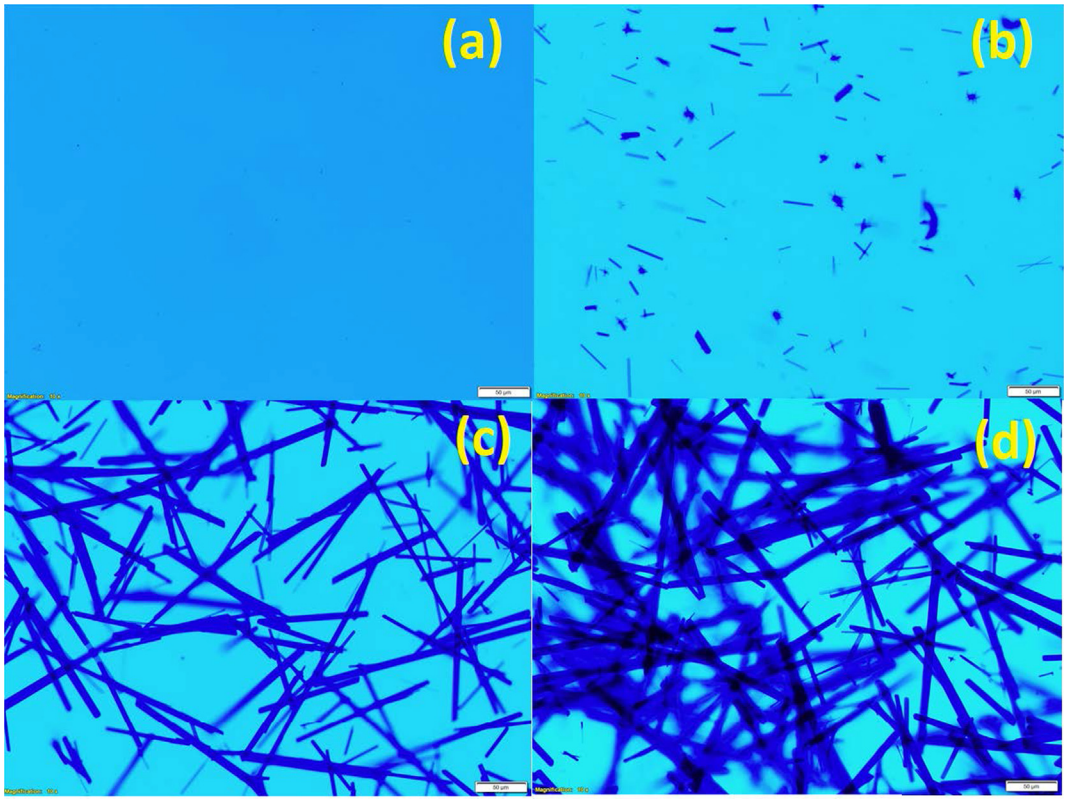

Fig. 3. Optical images of 0.06 g asphaltene in solution (a) completely dissolved asphaltene in toluene, (b) asphaltene particles formation in solution (4 vol.% hexane), (c) onset of asphaltene aggregation (12 vol.% hexane), (d) excess aggregation (22 vol.% hexane). The length scale of optical images is 50 μm as indicated in each of the sub figures.

the range of 1700–1550 cm^{-1} due to the carbonyl (C = O) stretching as shown in Fig. 6. Similar to our work, Cyran et al. [22] probed the 2D infrared spectra of Violanthrone-79 compound and used carbonyl stretching vibrational modes (1700–1550 cm^{-1}) to explain the aggregation effects. It is evident from the spectra that there is a difference in the transmittance among peaks present at the same wavenumber. This difference in the peak intensities can be explained by the presence of solid aggregates in the solution. In general, the blue line in the figure has maximum peak intensities across the considered range of wavenumber indicating the presence of maximum number of solid aggregates owing to the presence of the highest amount of n-hexane in the solution. The increase in the concentration of n-hexane in solution leads to pronounce formation of the aggregates. As the concentration of n-hexane reduces in the solution, the peak intensities reduce as depicted by the green line in the figure. To briefly summarize, the peak intensities keep on increasing as more number of aggregates start to precipitate out of the solution.

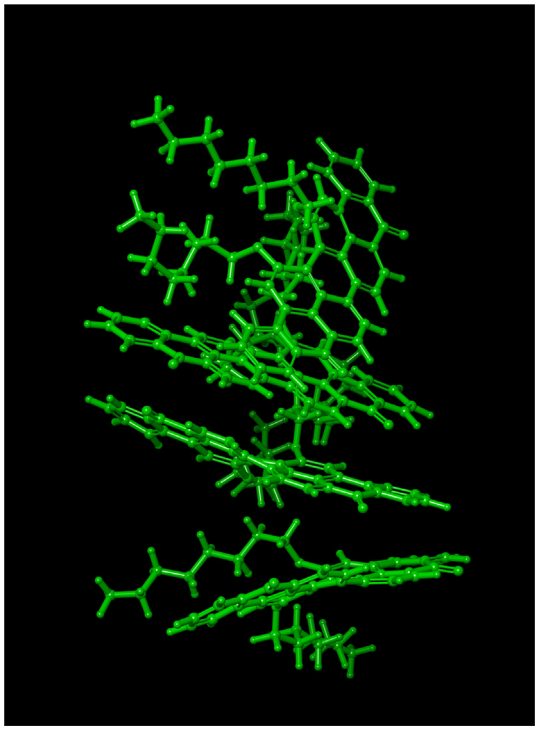

Fig. 4. A single aggregate of Violanthrone-79 in toluene and n-hexane mixture is shown for 36 asphaltene molecules. For clear visibility of the stacking arrangement, toluene and n-hexane are hidden.

Table 2
The average length and thickness of asphaltene particles as calculated from the optical images at the key steps are presented for 0.06 g asphaltene in solution.

Key steps	Length (μm)	Thickness (μm)
before on-set	30.95	2.43
at on-set	164.03	6.55
after on-set	168.28	10.86

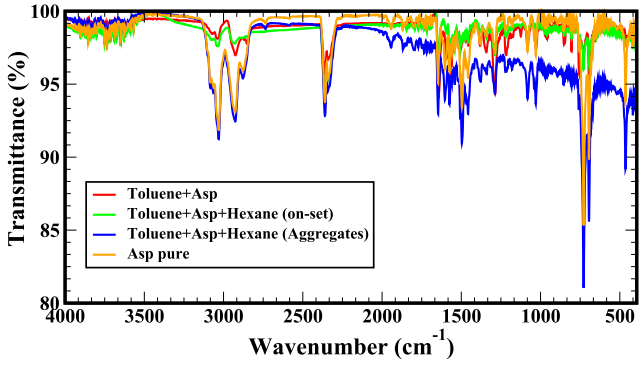

Fig. 5. FTIR spectra of the samples are shown. The red line represents fully dissolved asphaltene in toluene, the green line is for asphaltene-toluene mixture after the addition of the hexane (on-set of aggregation), the blue line represents asphaltene-toluene mixture with the excess amount of hexane (aggregation is evident) and the orange line denotes pure asphaltene sample.

4.3. Interaction Energy between Asphaltene-Toluene and Asphaltene-Hexane

We have investigated the total interaction energy to understand the asphaltene interaction with the solvent molecules. The total interaction energy is evaluated as the sum of the non-bonded

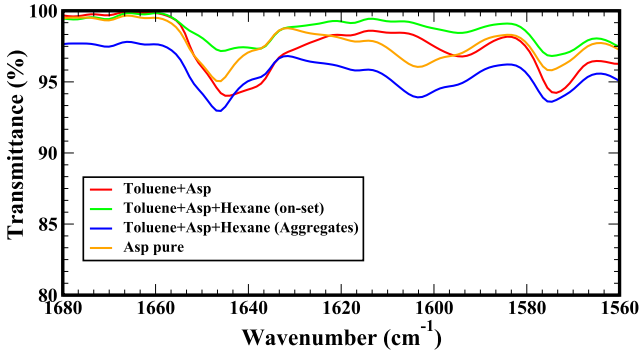

Fig. 6. FTIR spectra of the four samples are shown in the range of 1680–1560 cm^{-1}. The red line represents fully dissolved asphaltene in toluene, the green line denotes asphaltene-toluene mixture after the addition of the hexane (on-set of aggregation), the blue line is for asphaltene-toluene mixture with excess amount of the hexane (aggregation is evident) and the orange line denotes pure asphaltene sample.

interactions, i.e., electrostatic and van der Waals (vdW) interaction energies. The electrostatic and vdW interaction energies evaluated for different pairs of molecules are summarized in Table 3. The time-averaged electrostatic and van der Waals interaction energies between asphaltene-toluene are found to be −0.009258 kJ/mol and −0.10296 kJ/mol, respectively, in 36 asphaltene molecule system. The corresponding energies between asphaltene-hexane are −0.00068 kJ/mol and −0.23155 kJ/mol, respectively. The total interaction energy, which is the sum of the electrostatic and van der Waals interaction energies for asphaltene-toluene and asphaltene-hexane, are found to be −0.112 kJ/mol and −0.232 kJ/mol, respectively. The corresponding energies for 12 and 60 asphaltene molecules can be found in the Table 3.The negative total interaction energies for all three cases suggest attractive interactions among the different pairs of molecules considered within the study. The total interaction energy value of asphaltene-toluene indicates weaker attraction with respect to asphaltene-hexane. It is worthwhile to mention here that, Yaseen et al. [39] studied the interaction energy of asphaltene with solvents like ortho-xylene and water. It is observed within the study that there is a weak attractive interaction between asphaltene and ortho-xylene, whereas strong attractive interaction is observed between asphaltene and water.

4.4. End-to-End Distance

The distance between one end of the aliphatic side chain to the other end is termed as the end-to-end distance. This distance is crucial in understanding the aggregation behaviour of asphaltenes in aqueous solution as established by one of our previous works [40]. In this study, we probed the end-to-end distance to understand the aggregation behavior of asphaltenes in hexane and toluene mixture considering the semi-flexible side chains [41] within the worm-like chain model [42]. The end-to-end distance of the asphaltene molecule averaged over all asphaltene molecules is evaluated over the entire MD production run using the following Eq. 2 [41,40]:

$$\left\langle h^2 \right\rangle = 2L_P L_0[1 - (L_P/L_0)(1 - exp(-L_0/L_P))] \quad (2)$$

Here $\left\langle h^2 \right\rangle$ is the mean squared end-to-end distance, L_P is the persistence length and L_0 is the extended chain length.

Fig. 7(a) shows the averaged end-to-end distance for 12 asphaltene molecules as a function of time which varies between 8–15 Å. Fig. 7(b) shows a histogram of the mean end-to-end distances over all 12 asphaltene molecules in 10 ns simulation run. It is evident

Table 3
The average interaction energies between asphaltene-toluene and asphaltene-hexane pairs in three different asphaltene concentrations are presented below.

Interaction Pair	Asphaltene-Toluene		Asphaltene-Hexane	
	Electrostatic	van der Waals	Electrostatic	van der Waals
	12 Asphaltene molecules system			
Interaction Energy (kJ/mol)	−0.01016	−0.07840	-0.00138	−0.50652
Total Interaction Energy (kJ/mol)	-0.089		-0.508	
	36 Asphaltene molecules system			
Interaction Energy (kJ/mol)	−0.00926	−0.10296	−0.00068	−0.23155
Total Interaction Energy (kJ/mol)	-0.112		-0.232	
	60 Asphaltene molecules system			
Interaction Energy (kJ/mol)	−0.000217	−0.002191	−0.00352	−0.84035
Total Interaction Energy (kJ/mol)	-0.00241		-0.844	

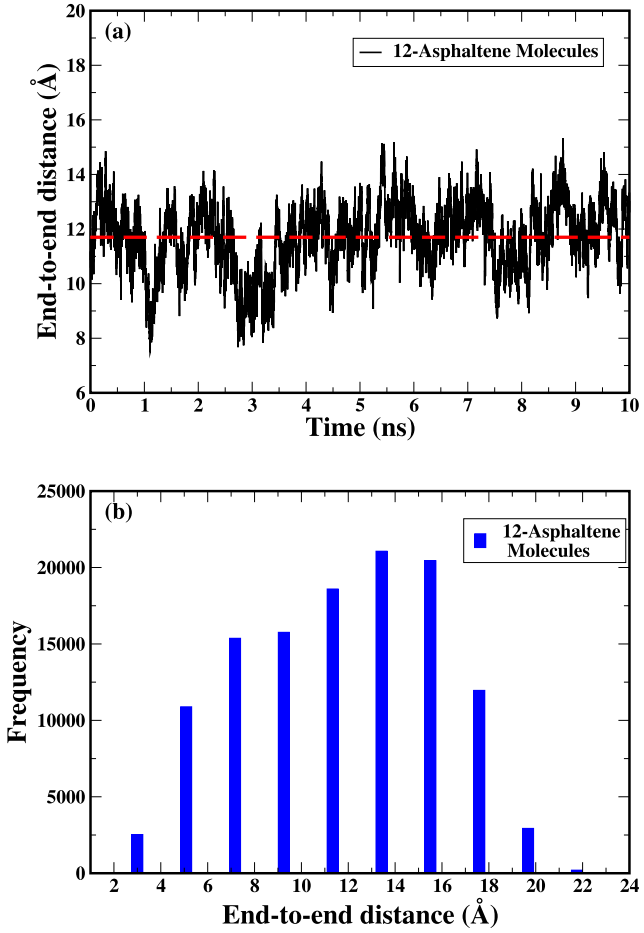

Fig. 7. (a) Time series of end-to-end distance of asphaltene molecules is shown for the 10 ns of the production run for 12 asphaltene molecules in toluene-hexane mixture. (b) Frequency as a function of mean end-to-end distances over all molecules is shown for 12 asphaltene molecules in toluene-hexane mixture.

from the figure that the maximum frequency is at the end-to-end distance of 13.42 Å, whereas the averaged end-to-end distance is found to be 11.7 Å. The end-to-end distance and the persistence length for the three different asphaltene concentrations under investigation are summarized in Table 4. The extended chain length for asphaltene is found to be 24.5 Å. The aliphatic side-chains can change the persistence length in aqueous solution [40] and in organic solvents. The stiffer aliphatic side chains are found on shorter length scales and the longer length scale side chains bend to participate in the aggregation process. The end-to-end distance of the asphaltene molecules is approximately same and within the standard deviation limit with respect to the concentration of asphaltene in toluene-hexane mixture. Our results clearly show the aggregation of asphaltene molecules in toluene-hexane mixture and that the aggregate size increases with increase in the hexane concentration. Further, a persistence length of approximately 3.6 Å is observed for the all the considered concentrations. This length indicates that beyond this distance there will be no correlation, i.e., the aliphatic side chains are stiff for ca. 3.6 Å. This is due to the fact that formed aggregates are stable and no frequent disaggregation is observed during the production run.

4.5. Density Contours

The asphaltene aggregate cross-section contours are calculated by taking layers of a specified thickness perpendicular to a selected axis. The cross-section density is evaluated using the layer partitioned into cubes. The volume fraction of each atom that overlaps each cube is determined and weighted by the atomic mass, summed and divided by the cube volume to obtain the density in the cube.

The asphaltene aggregate densities for three different concentrations are shown in Fig. 8. The density contour for 12 asphaltene molecules is shown in Fig. 8 (top). The middle and bottom subfigures of Fig. 8 show density contours for 36 and 60 asphaltene molecules, respectively. It is evident from the figure that the asphaltene aggregates are delocalized for the highest asphaltene concentration considered within the study, whereas for the lowest concentration, these aggregates are localized.

4.6. Diffusion Coefficient

The diffusion coefficient of the asphaltene molecules is evaluated using the following Eq. 3 [43]:

$$D = \frac{1}{6}\lim_{t\to\infty}\frac{d}{dt}\left\langle|\vec{r}(t)-\vec{r}(0)|^2\right\rangle \tag{3}$$

where $\left\langle|\vec{r}(t)-\vec{r}(0)|^2\right\rangle$ is the mean-square displacements. The calculated diffusion coefficients are presented in Table 5 for the considered concentrations of asphaltene. There is a clear trend that the diffusion coefficient decreases with increase in the asphaltene concentration in hexane and toluene mixture. This observation can be explained by the restricted motion of asphaltene molecules owing to the formation of several aggregates at high asphaltene concentrations which is supported by the density contours for different asphaltene concentrations as discussed before.

Table 4
The calculated end-to-end distance, persistence length, extended chain length (in Å) averaged over 10 ns of production run, the standard deviation of time series and molecular distribution standard deviation (Å) with respect to three considered asphaltene concentrations are presented in the table.

Concentration	End-to-end distance (Å)	Persistence length (Å)	Extended chain length (Å)	Time series standard deviation (Å)	Molecular distribution standard deviation (Å)
12 Asphaltene Molecules	11.70	3.69	24.5	1.24	4.12
36 Asphaltene Molecules	11.57	3.60	24.5	0.69	4.13
60 Asphaltene Molecules	11.49	3.54	24.5	0.50	4.10

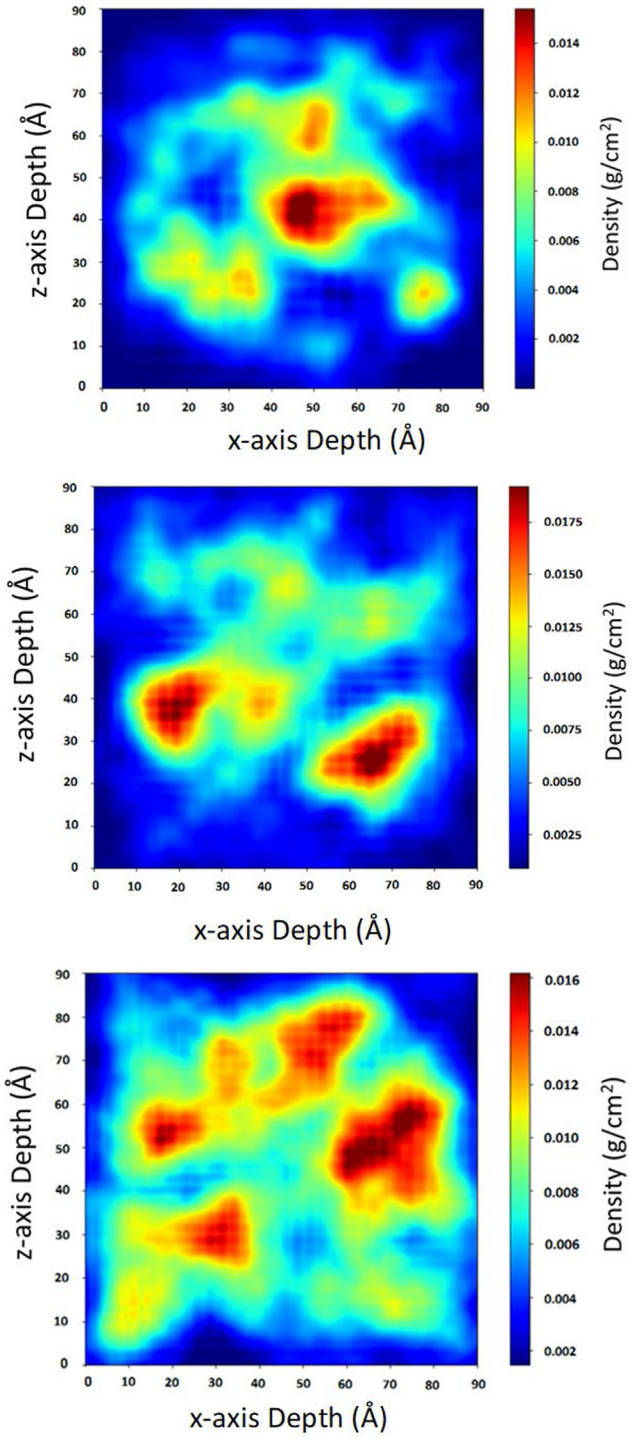

Fig. 8. The density contours for (top) 12, (middle) 36, and (bottom) 60 asphaltene molecules in toluene-hexane mixture are shown in the figure.

Table 5
The obtained diffusion coefficients (in m^2/s) of asphaltene in toluene and hexane mixture along with the standard deviation (σ) are presented in the table.

Concentration	Diffusion Coefficient (m^2/s)	σ (m^2/s)
12 Asphaltene Molecules	6.55×10^{-10}	2.15×10^{-13}
36 Asphaltene Molecules	4.94×10^{-10}	7.70×10^{-13}
60 Asphaltene Molecules	3.38×10^{-10}	2.49×10^{-13}

4.7. Viscosity

Finally, we calculated the shear viscosity of the solution using MD simulations in association with the Green–Kubo formalism as given by the following Eq. 4 [44]:

$$\eta = \frac{V}{k_B T}\int_0^\infty \langle P_{\alpha\beta}(t) \bullet P_{\alpha\beta}(0)\rangle dt. \quad (4)$$

where V is the volume of the system, k_B is the Boltzmann constant, T is the temperature and $P_{\alpha\beta}$ is the off-diagonal pressure tensor.

In order to calculate the viscosity, 25 independent MD runs are performed starting with different atomic velocities. The viscosity as function of time is calculated at each MD simulation run using the obtained pressure tensor. The average viscosity curve is obtained by averaging over multiple viscosity curves and then an exponential function is used to fit the average curve data. The asymptote of the fitted functions is considered as the final shear viscosity. The viscosities for the three different asphaltene concentrations are summarized in Table 6. The viscosity values of 0.43 cP, 0.52 cP and 0.61 cP are obtained for 12, 36 and 60 asphaltene molecule systems in toluene and hexane mixture, respectively. Our results clearly show that there is an increase in the viscosity with increase in the asphaltene concentration.

5. Conclusion

In this study, the aggregation behaviour of asphaltene (Violanthrone-79) in toluene-hexane mixture is thoroughly investigated by combining experiments with MD simulations. Both experiments and the MD simulations support formation of the 1D rod-like aggregates. From the optical images, it is clear that with an increase in the concentration of the titrant (n-hexane), the stacking of the aggregates become non-directional and an increase in the thickness of the aggregates is observed. FTIR spectra show an increase in the intensity of the peaks after formation of

Table 6
The obtained viscosities (in cP) along with the standard deviation of the fit (σ) for asphaltene in toluene-hexane mixture for the three different concentrations are presented in the table.

Concentration	Viscosity (cP)	σ (cP)
12 Asphaltene Molecules	0.43	0.036
36 Asphaltene Molecules	0.52	4.39×10^{-5}
60 Asphaltene Molecules	0.61	0.03016

the aggregates and also a clear increase in the carbonyl (C = O) stretching intensity in the presence of aggregates. The uniform end-to-end distances of asphaltene molecules at considered concentrations indicate that the end-to-end distance is purely solvent dependent and also suggests that the aggregates are stable. Our theoretical investigations clearly show that with increase in the concentration of asphaltene, larger and numerous nano-aggregates are formed as evident from the density contours. We also observe that the increase in concentration of the asphaltene leads to decrease in the diffusion coefficient. Finally, the obtained viscosity values increase with the rise in the asphaltene concentration and the solution with lowest viscosity indeed has the highest diffusion coefficient of asphaltenes due to the presence of lesser number of aggregates in the solution.

Declaration of Competing Interest

The authors declare that they have no known competing financial interests or personal relationships that could have appeared to influence the work reported in this paper.

Acknowledgments

The authors would like to express their gratitude to Schrödinger Centre for Molecular Simulations, MAHE, Manipal for their support. Laxman Kumar Kundarapu would like to thank MAHE, Manipal for research seed grant (reference number: 00000388).

References

[1] T.F. Yen, Asphaltenes, Springer US, Boston, MA, 1998, pp. 1–20. URL https://doi.org/10.1007/978-1-4899-1615-0_1
[2] P. Spiecker, K.L. Gawrys, P.K. Kilpatrick, Aggregation and solubility behavior of asphaltenes and their subfractions, J. Colloid Interface Sci. 267 (1) (2003) 178–193, http://www.sciencedirect.com/science/article/pii/S0021979703006416.
[3] D.L. Mitchell, J.G. Speight, The solubility of asphaltenes in hydrocarbon solvents, Fuel 52 (2) (1973) 149–152, http://www.sciencedirect.com/science/article/pii/0016236173900409.
[4] T.F. Yen, J.G. Erdman, S.S. Pollack, Investigation of the structure of petroleum asphaltenes by x-ray diffraction, Anal. Chem. 33 (11) (1961) 1587–1594, https://doi.org/10.1021/ac60179a039.
[5] J. Sjöblom, N. Aske, I.H. Auflem, T.E. Øystein Brandal, Øystein Sæther Havre, A. Westvik, E.E. Johnsen, H. Kallevik, Our current understanding of water-in-crude oil emulsions.: Recent characterization techniques and high pressure performance, Adv. Colloid Interface Sci. 100–102 (2003) 399–473, http://www.sciencedirect.com/science/article/pii/S0001868602000660..
[6] C. Pierre, L. Barré, A. Pina, M. Moan, Composition and heavy oil rheology, Oil and Gas Science and Technology-revue De L Institut Francais Du Petrole - OIL GAS SCI TECHNOL 59 (2004) 489–501.
[7] K. Akbarzadeh, A. Hammami, A. Kharrat, D. Zhang, S. Allenson, J. Creek, S. Kabir, A. Jamaluddin, A. Marshall, R. Rodgers, O. Mullins, T. Solbakken, Asphaltenes - problematic but rich in potential, Oilfield Rev. 19 (2007) 22–43.
[8] E.Y. Sheu, O.C. Mullins, Asphaltenes: fundamentals and applications, 1995.
[9] I. Merdrignac, D. Espinat, Physicochemical characterization of petroleum fractions: the state of the art, Oil and Gas Science and Technology - Revue de l'IFP 62 (2007) 7–32.
[10] S. Ilyin, M. Arinina, M. Polyakova, G. Bondarenko, I. Konstantinov, V. Kulichikhin, Asphaltenes in heavy crude oil: Designation, precipitation, solutions, and effects on viscosity, J. Pet. Sci. Eng. 147 (2016) 211–217.
[11] Z. Rashid, C.D. Wilfred, N. Gnanasundaram, A. Arunagiri, T. Murugesan, A comprehensive review on the recent advances on the petroleum asphaltene aggregation, J. Pet. Sci. Eng. 176 (2019) 249–268, http://www.sciencedirect.com/science/article/pii/S0920410519300063.
[12] M. Szymula, A. Marczewski, Adsorption of asphaltenes from toluene on typical soils of lublin region, Appl. Surf. Sci. 65 (2002) 301–311.
[13] X. Zhu, D. Chen, G. Wu, Molecular dynamic simulation of asphaltene co-aggregation with humic acid during oil spill, Chemosphere 138 (2015) 412–421.
[14] E. Joonaki, J. Buckman, R. Burgass, B. Tohidi, Water versus asphaltenes; liquid-liquid and solid-liquid molecular interactions unravel the mechanisms behind an improved oil recovery methodology, Sci. Rep. 9 (11369) (2019) 1–5.
[15] O. Mullins, H. Sabbah, J. Eyssautier, A. Pomerantz, L. Barré, A. Andrews, Y. Ruiz-Morales, F. Mostowfi, R. McFarlane, L. Goual, R. Lepkowicz, T. Cooper, J. Orbulescu, R. Leblanc, J. Edwards, R. Zare, Advances in asphaltene science and the yen-mullins model, Energy Fuels 26 (2012) 3986–4003.
[16] J.S. Buckley, Asphaltene deposition, Energy Fuels 26 (7) (2012) 4086–4090, https://doi.org/10.1021/ef300268s.
[17] X. Li, Y. Guo, E.S. Boek, X. Guo, Experimental study on kinetics of asphaltene aggregation in a microcapillary, Energy Fuels 31 (9) (2017) 9006–9015, https://doi.org/10.1021/acs.energyfuels.7b01170.
[18] T. Takanohashi, S. Sato, I. Saito, R. Tanaka, Molecular dynamics simulation of the heat-induced relaxation of asphaltene aggregates, Energy Fuels 17 (2002) 135–139.
[19] T.F. Headen, E.S. Boek, N.T. Skipper, Evidence for asphaltene nanoaggregation in toluene and heptane from molecular dynamics simulations, Energy Fuels 23 (3) (2009) 1220–1229, https://doi.org/10.1021/ef800872g.
[20] J. Eyssautier, P. Levitz, D. Espinat, J. Jestin, J. Gummel, I. Grillo, L. Barré, Insight into asphaltene nanoaggregate structure inferred by small angle neutron and x-ray scattering, J. Phys. Chem. B 115 (21) (2011) 6827–6837, pMID: 21553910. doi: 10.1021/jp111468d.
[21] S. Aslan, A. Firoozabadi, Effect of water on deposition, aggregate size, and viscosity of asphaltenes, Langmuir 30 (13) (2014) 3658–3664, pMID: 24650340. doi: 10.1021/la404064t.
[22] J.D. Cyran, A.T. Krummel, Probing structural features of self-assembled violanthrone-79 using two dimensional infrared spectroscopy, J. Chem. Phys. 142 (21) (2015) 212435, https://doi.org/10.1063/1.4919637.
[23] B. Schuler, G. Meyer, D. Peña, O.C. Mullins, L. Gross, Unraveling the molecular structures of asphaltenes by atomic force microscopy, J. Am. Chem. Soc 137 (31) (2015) 9870–9876, pMID: 26170086. doi: 10.1021/jacs.5b04056.
[24] L. Zhang, C. Shi, Q. Lu, Q. Liu, H. Zeng, Probing molecular interactions of asphaltenes in heptol using a surface forces apparatus: Implications on stability of water-in-oil emulsions, Langmuir 32 (19) (2016) 4886–4895, pMID: 27128395. doi: 10.1021/acs.langmuir.6b01000.
[25] J.A. Duran, Y.A. Casas, L. Xiang, L. Zhang, H. Zeng, H.W. Yarranton, Nature of asphaltene aggregates, Energy & Fuels 33 (5) (2019) 3694–3710, https://doi.org/10.1021/acs.energyfuels.8b03057.
[26] H. Santos Silva, A. Alfarra, G. Vallverdu, D. Bégué, B. Bouyssiere, I. Baraille, Asphaltene aggregation studied by molecular dynamics simulations: role of the molecular architecture and solvents on the supramolecular or colloidal behavior, Pet. Sci. 16 (2019) 669–684.
[27] C. Jian, T. Tang, S. Bhattacharjee, Molecular dynamics investigation on the aggregation of violanthrone78-based model asphaltenes in toluene, Energy & Fuels 28 (6) (2014) 3604–3613, https://doi.org/10.1021/ef402208f.
[28] C. Jian, T. Tang, Molecular dynamics simulations reveal inhomogeneity-enhanced stacking of violanthrone-78-based polyaromatic compounds in n-heptane-toluene mixtures, The Journal of Physical Chemistry B 119 (27) (2015) 8660–8668, pMID: 26076902. doi: 10.1021/acs.jpcb.5b04481.
[29] J. Wang, A.L. Ferguson, Mesoscale simulation of asphaltene aggregation, The Journal of Physical Chemistry B 120 (32) (2016) 8016–8035, pMID: 27455391. doi: 10.1021/acs.jpcb.6b05925.
[30] H. Bian, A. Kan, Z. Yao, Z. Duan, H. Zhang, S. Zhang, L. Zhu, D. Xia, Impact of functional group methylation on the disaggregation trend of asphaltene: A combined experimental and theoretical study, J. Phys. Chem. C 123 (49) (2019) 29543–29555, https://doi.org/10.1021/acs.jpcc.9b07695.
[31] A. Tirjoo, B. Bayati, H. Rezaei, M. Rahmati, Molecular dynamics simulations of asphaltene aggregation under different conditions, J. Pet. Sci. Eng. 177 (2019) 392–402, http://www.sciencedirect.com/science/article/pii/S0920410519301780.
[32] B.S. Soulgani, F. Reisi, F. Norouzi, Investigation into mechanisms and kinetics of asphaltene aggregation in toluene/n-hexane mixtures, Petroleum Science 17 (2020) 457–466.
[33] T. Sato, S. Araki, M. Morimoto, R. Tanaka, H. Yamamoto, Comparison of hansen solubility parameter of asphaltenes extracted from bitumen produced in different geographical regions, Energy & Fuels 28 (2) (2014) 891–897, https://doi.org/10.1021/ef402065j.
[34] W.E.M. Schermer, P.M.J. Melein, F.G.A. van den Berg, Simple techniques for evaluation of crude oil compatibility, Pet. Sci. Technol. 22 (7–8) (2004) 1045–1054, https://doi.org/10.1081/LFT-120038695.
[35] E. Harder, W. Damm, J. Maple, C. Wu, M. Reboul, J.Y. Xiang, L. Wang, D. Lupyan, M.K. Dahlgren, J.L. Knight, J.W. Kaus, D.S. Cerutti, G. Krilov, W.L. Jorgensen, R. Abel, R.A. Friesner, Opls3: A force field providing broad coverage of drug-like small molecules and proteins, J. Chem. Theory Comput. 12 (1) (2016) 281–296, pMID: 26584231. doi: 10.1021/acs.jctc.5b00864.
[36] K.J. Bowers, E. Chow, H. Xu, R.O. Dror, M.P. Eastwood, B.A. Gregersen, J.L. Klepeis, I. Kolossvary, M.A. Moraes, F.D. Sacerdoti, J.K. Salmon, Y. Shan, D.E. Shaw, Scalable algorithms for molecular dynamics simulations on commodity clusters, in: Proceedings of the 2006 ACM/IEEE Conference on Supercomputing, SC '06, ACM, New York, NY, USA, 2006. URL http://doi.acm.org/10.1145/1188455.1188544
[37] SchrÖdinger release 2018, in: SchrÖdinger Release 2018, SchrÖdinger, LLC, New York, NY, 2018.
[38] J.C. Franco, G. Goncalves, M.S. Souza, S.B.C. Rosa, L.M. Thiegue, T.D.Z. Atvars, P. T.V. Rosa, R.A. Nome, Towards in situ fluorescence spectroscopy and microscopy investigations of asphaltene precipitation kinetics, Opt. Express 21 (25) (2013) 30874–30885, http://www.opticsexpress.org/abstract.cfm?URI=oe-21-25-30874.
[39] S. Yaseen, G.A. Mansoori, Molecular dynamics studies of interaction between asphaltenes and solvents, J. Petrol. Sci. Eng. 156 (2017) 118–124, https://www.sciencedirect.com/science/article/pii/S0920410517304916.
[40] A.K. Vatti, A. Caratsch, S. Sarkar, L.K. Kundarapu, S. Gadag, U.Y. Nayak, P. Dey, Asphaltene aggregation in aqueous solution using different water models: A classical molecular dynamics study, ACS Omega 5 (27) (2020) 16530–16536, https://doi.org/10.1021/acsomega.0c01154.

[41] S. Brinkers, H.R.C. Dietrich, F.H. de Groote, I.T. Young, B. Rieger, The persistence length of double stranded dna determined using dark field tethered particle motion, J. Chem. Phys. 130 (21) (2009) 215105, https://doi.org/10.1063/1.3142699.
[42] J.N. Milstein, J.-C. Meiners, Worm-Like Chain (WLC) Model, Springer, Berlin Heidelberg, Berlin, Heidelberg, 2013, pp. 2757–2760. doi: 10.1007/978-3-642-16712-6_502.
[43] Understanding molecular simulation: From algorithms to applications, in: D. Frenkel, B. Smit (Eds.), Understanding Molecular Simulation (Second Edition), second edition Edition, Academic Press, San Diego, 2002.
[44] A.M.P., Computer simulations of liquids, oxford University Press, Oxford, 1987.